PCCP

Accepted Manuscript

ROYAL SOCIETY OF CHEMISTRY

www.rsc.org/pccp

Journal Name

RSCPublishing

ARTICLE

Molecular Dynamics Study of Model SI Clathrate Hydrates: Effect of Guest Size and Guest-Water Interaction on Decomposition Kinetics

Cite this: DOI: 10.1039/x0xx00000x

Received 00th January 2012,
Accepted 00th January 2012

DOI: 10.1039/x0xx00000x

www.rsc.org/

Subhadip Das,[a] Vikesh Singh Baghel,[b] Sudip Roy,*[a] Rajnish Kumar*[b]

One of the options suggested for methane recovery from natural gas hydrates are molecular replacement of methane by a suitable guests like CO_2 and N_2. This approach has been found feasible through many experimental and molecular dynamics simulation studies. However, long term stability of resulting hydrate needs to be evaluated; the decomposition rate of these hydrates is expected to depend on the interaction between these guest and water molecules. In this work, molecular dynamics simulation has been performed to illustrate the role of guest molecules with different size and interaction strength with water on structure I (SI) hydrate decomposition and hence the stability. The van der Waals interaction between water of hydrate cages and guest molecules are defined by Lennard Jones potential parameters. A wide range of parameter space has been scanned by changing the guest molecules in SI hydrate which acts as a model gas for occupying the small and large cages of SI hydrate. All atomistic simulation result shows that the stability of hydrate is sensitive to the size and interaction of the guest molecules with hydrate water. Increase in interaction of guest molecules with water stabilizes the hydrate, which in turn shows slower rate of hydrate decomposition. Similarly guest molecules with reasonably small (similar to Helium) or large size increases the decomposition rate. Results were also analyzed by calculating structural order parameter to understand the dynamics of crystal structure and correlated with the release rate of guest molecules from solid hydrate phase. Results have been explained on the basis of calculation of potentials energies felt by guest molecules in amorphous water, hydrate bulk and hydrate-water interface region.

Introduction

Gas hydrates are crystalline non-stoichiometric inclusion compounds comprised of organic/inorganic moieties trapped within the cavities of a rigid cage-like lattice of water molecules.[1] The individual cages are stabilized by dispersion interactions between the trapped (enclathrated) guest molecule and the surrounding water molecules forming the hydrate lattice. Hydrate structures are classified into three categories; cubic SI, cubic structure II (SII) and hexagonal structure H (SH) based on the geometries of their constituent water molecules. The SI unit cell has two 5^{12} (pentagonal dodecahedron) and six $5^{12}6^2$ (hexagonal truncated trapezohedron) cages; similarly, the SII unit cell has sixteen 5^{12} and eight $5^{12}6^4$ cages, and SH has three 5^{12}, two $4^3 5^6 6^3$, and one $5^{12}6^8$ cages[2]. At moderate temperature and pressure it is expected that each cage can occupy one guest molecule.

Gas hydrates for the first time was identified by Sir Humphery Davy in 1811, which remained an academic curiosity for most part of nineteenth century. However, it has been studied extensively in last few decades not only because of its complex structural and chemical properties[3] but also due to its importance in flow assurance and methane recovery from natural gas hydrate reserves.[4] Potential recovery of methane from the natural gas hydrate reserves scattered along the continental offshore margins and in permafrost regions has attracted significant interest in the study of methane hydrate formation and decomposition dynamics.[5, 6] Additionally researchers have looked into possible applications of gas hydrates in molecular hydrogen storage[7-13], desalination of water[14, 15] and carbon dioxide capture[16, 17].

The practical applications of gas hydrates in several fields are subjected to their stability at the operating conditions. The size of guest molecule as well as its interaction with neighboring crystalline water molecules plays an important role in determining the thermodynamic stability of a preferred hydrate structure depending on the surrounding pressure and temperature conditions.[6, 18-26] Hydrate forming guest molecules range from sizes as small as hydrogen, methane and carbon dioxide to as large as tetrahydrofuran, cyclopentane and neo-hexane. Similarly, the guest molecule also differs in the magnitude of their polarity and solubility in water. This aspect has not received much attention as mostly it is sufficient to

measure hydrate stability for required application. One of the approaches suggested for methane recovery from natural gas hydrate is molecular substitution. CO_2 hydrate is thermodynamically more stable compared to CH_4 hydrate and thus it has been proposed that it would be thermodynamically feasible to replace methane by CO_2. However, not much work has been done into long term stability of resultant SI hydrate compared to pure methane hydrate which is more of less stable from several centuries.

Literature suggests that quite a few studies has been done which correlate the guest molecule size and resulting stable structure of gas hydrate at moderate temperature and pressure. [18, 27-32] In a recent study, Schicks et al[28] applied DSC in combination with XRPD to calculate the dissociation enthalpies of single and multicomponent gaseous hydrates of pure methane as well as methane-carbon dioxide and methane-ethane-propane mixtures. They have found that as the methane in the large cages get replaced by guest molecule of larger sizes, the molar dissociation of enthalpy increases. This is due to increase in the interaction between guest and host molecule or in other words, the stability of the hydrates enhanced on increasing the molecular size of guest molecules. Tezuka et al[27] found a correlation between the size and conformation of guest molecule(LMGS) on the thermodynamic stability and crystal lattice parameters of structure H (SH) hydrate . The authors showed that the thermodynamic stability not only depends on the size of the guest molecules but also on the tilt angle and dihedral angle distribution of the guest molecule trapped inside the cage. The equilibrium conditions for a stable hydrate structure also depend on the molecular size of guest to cage diameter ratio. Below a ratio of about 0.76, the molecular attractive forces contribute less to cavity stability. Above the upper bound ratio of about 1.0, the guest molecule cannot fit into a cavity without distorting the cage.[26] Zhao et al [33]simulated the dissociation behavior of carbon dioxide, methane and hydrogen hydrate and found out that the activation barrier to the dissociation of carbon dioxide and methane hydrate compared to hydrogen hydrate is quite higher. This can be attributed to the small size of hydrogen as compared to methane and carbon dioxide.

With the advances in computational power in recent times, molecular simulations have played a key role in understanding the properties of gas hydrate systems at the molecular level. Researchers in the field of gas hydrates have applied several molecular simulation techniques like Monte Carlo (MC), Density Functional Theory (DFT) and Molecular Dynamics (MD).[34-47] Jiang and Jordan[48] compared the properties of Xe, CH_4, and CO_2 hydrates by molecular dynamics (MD) simulations. From the guest molecule-water interaction energy, the authors have pointed out that host-guest coupling plays a significant role in stabilizing CO_2 hydrate than Xe or CH_4 hydrate. They also suggested that CO_2 and Xe hydrate have lower speeds of sound and thermal conductivity values than CH_4 hydrate due to the increased host-guest coupling. Several MD and MC simulation studies of dissociation of single component gas hydrate such as methane[37, 45, 47, 49, 50] , carbon dioxide[51, 52] have been reported. A number of data has been published on the stability of hydrates with various guest molecules, but still there is no comprehensive understanding regarding the correlation between the stability of hydrates and the nature (size and interaction strength) of guest molecules. In this work, suitable MD simulations were done to explore systematically how the properties of guest molecules in fully occupied SI type hydrate cages affect the rate of hydrate decomposition. Lennard Jones (LJ) potential was used to calculate the non-bonded interactions between the particles (atom/molecules). As the size of the particle while using LJ potential is defined by sigma and the hydrophobicity/ hydrophilicity is governed by epsilon parameter, the stability of the SI hydrate cages were checked with varying epsilon and sigma values. Both the terms hydrophobicity and hydrophilicity may be coined relatively to depict whether the interaction between guest molecules and the hydrate water molecules is favorable or not compared to methane hydrate. So, whenever the interaction between water and guest molecules is higher than methane-water interaction one may refer to it as hydrophilic with respect to methane. The epsilon and sigma values were chosen so as to represent closely several hydrate forming molecules and an attempt was made to correlate the stability of SI hydrate structure with varying LJ parameters at different temperatures and 10 MPa pressure. The stability was determined by the number of guest molecules retained inside the cages, the potential energy curves and the four body order parameter. The computational details and simulation procedure are discussed in detail in the following sections.

Computational Details

Double-precision GROMACS[53] (version 4.5.5) code was used to perform simulations . The extended simple point charge [54] (SPC/E) model was used for water . Guest molecules are treated as united atom.

.

$$U_{ij}(r_{ij}) = 4\varepsilon_{ij}\left[\left(\frac{\sigma_{ij}}{r_{ij}}\right)^{12} - \left(\frac{\sigma_{ij}}{r_{ij}}\right)^{6}\right] \qquad (1)$$

$$\sigma_{ij}=\frac{\sigma_i+\sigma_j}{2} \qquad \epsilon_{ij}=\sqrt{\epsilon_i\epsilon_j}$$

where ϵ ,the depth of the potential well can be related to the interaction strength of guest molecules in water and σ to the diameter (size) of guest molecule. In general, the chosen LJ parameters of different guest molecules cover a wider range, related closely to various guest molecules that can form hydrate. The LJ parameters of the guest molecule used in this study are represented in **Figure 1**. The Lorentz-Berthelot combination[55] rules was used to determine the parameters of the LJ interaction between the water and methane molecules. Ewald [56] summations was used to account for long-range electrostatic interactions. The Fourier part of the Ewald sums were evaluated by using the particle mesh Ewald method (PME) of Darden and co-workers [57, 58] with a relative Ewald tolerance of 1×10^{-6} . The unit cell of the methane hydrate was obtained from the literature[59, 60]. The methane hydrate crystal was comprised of structure I unit cells belonging to the cubic space group Pm3n with a lattice constant of 11.76 Å.

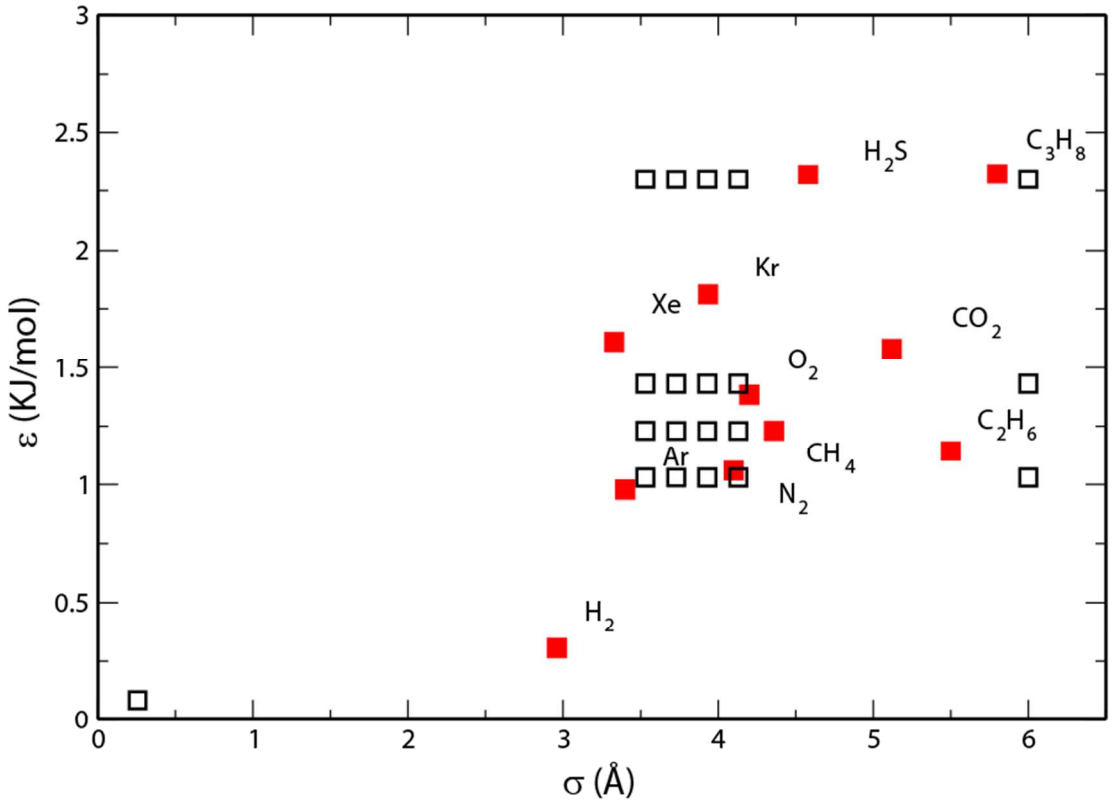

Figure 1. LJ parameters (black void squares) for guest molecules investigated in this work. To compare with experimental studies, the LJ parameters of some of the common guest molecules are also shown (red filled squares).

A 3×3×6 supercell was made with near zero dipole moment and thus satisfying Bernal Fowler ice rules[61]. The supercell containing a total of 54 unit cells was then used to constitute the initial hydrate phase to create the hydrate slab with two interfaces in the z direction. Incomplete open cages, which promote decomposition at the interfaces, were introduced at the interfaces. The crystalline symmetry was preserved at the two ends of the hydrate slab by taking complementary open cages at the interface. Liquid water consisting of 3027 water molecules at a density of 1g/cm^3 was introduced at both sides of the interface in the z direction constituting the initial amorphous or bulk phase making the final simulation box of the dimension 3.5 X 3.5 X 14.5 nm^3. The system finally consisted of 432 methane molecules out of which 108 were in small cages and 324 were in large cages, 2484 hydrate water molecules and 3027 bulk water outside the hydrate structure.

The leapfrog algorithm was used to integrate the equations of motion with a time step of 1 fs for canonical (NVT) and isobaric-isothermal (NPT) ensemble simulations (equilibration steps) and 0.5 fs for micro-canonical (NVE) simulations (production run). The smaller simulation time for NVE production run was chosen to reduce the error in total energy calculations and hence to maintain a constant total energy. Total energy plots of the NVE simulations for few systems are given in Figure S1 of ESI. NVE simulations were used so that the temperature change in the system can be monitored, as the hydrate decomposition process is an endothermic process. Shake algorithm was used to constrain the bond length between the atoms in rigid molecules (all molecules were taken as rigid) with a relative shake tolerance of 1×10^{-10}. Short-range nonbonded interactions between the molecules were calculated within a cutoff distance (R_{cut}) of 15.0 Å .

The simulation box under the periodic boundary conditions are equilibrated by following a generalized simulation procedure flowchart given in Figure S2 of ESI. All the systems were subjected to NVT and NPT runs for 6 ns and 1 ns respectively with position restrained hydrate phase for equilibrating the amorphous water. Further unrestrained NPT simulation was performed for 10 ps to equilibrate the hydrate phase to the potentials energy surface of the water and guest molecules. All these simulations were performed at 273 K and 10 MPa (for NPT runs). Due to the stepwise equilibration as reported above, the entire system was satisfactorily equilibrated at 273 K and 10 MPa to the potential energy surface of the classical force field used for the simulation. Nose−Hoover thermostat[63, 64] with coupling time constant of 0.5 ps and a Parrinello Rahman[65, 66] barostat with a coupling time constant of 2 ps were used for both the restrained and unrestrained NPT simulations. However to study the dissociation process by thermal energy we need to increase the temperature of the system. Therefore, to study the decomposition process at the higher temperatures of 310 K, simulated annealing was performed (for 14 ps) to increase the temperature gradually from 273 K to 310K. However we have observed some initiation of melting at the interface (between water and hydrate) even in this small simulated annealing time. The velocities of the atoms and input co-ordinates were taken

from the last step of equilibration (i.e. last NPT run at 273K) as an input. The output structure and velocities of molecules after the simulated annealing step were taken as input for the final NVE production runs at 310K. Both the LJ and Coulombic interaction potentials were shifted in case of NVE simulations with the switch starting at a distance of 1 Å before the R_{cut}[67] i.e, at 14 Å as implemented in GROMACS. This is mainly useful to keep energy constant for NVE simulations. Because of introduction of PME switch the short range Coloumbic potential used in NVE simulation is modified (i.e. shifted). The missing long range potential is properly calculated and added to PME. By introducing this switch function we ensure that the energy of the NVE runs gets conserved. Since it is important to converse energy in NVE run, we have only used the switch function in NVE runs, not in NVT/NPT runs. The NVE production runs were performed for 6 ns. All the simulations were repeated three times at a temperature of 310K, independent of previous run, to obtain properties with higher statistics. In the paper, we have given properties calculated from the simulations at 310K.

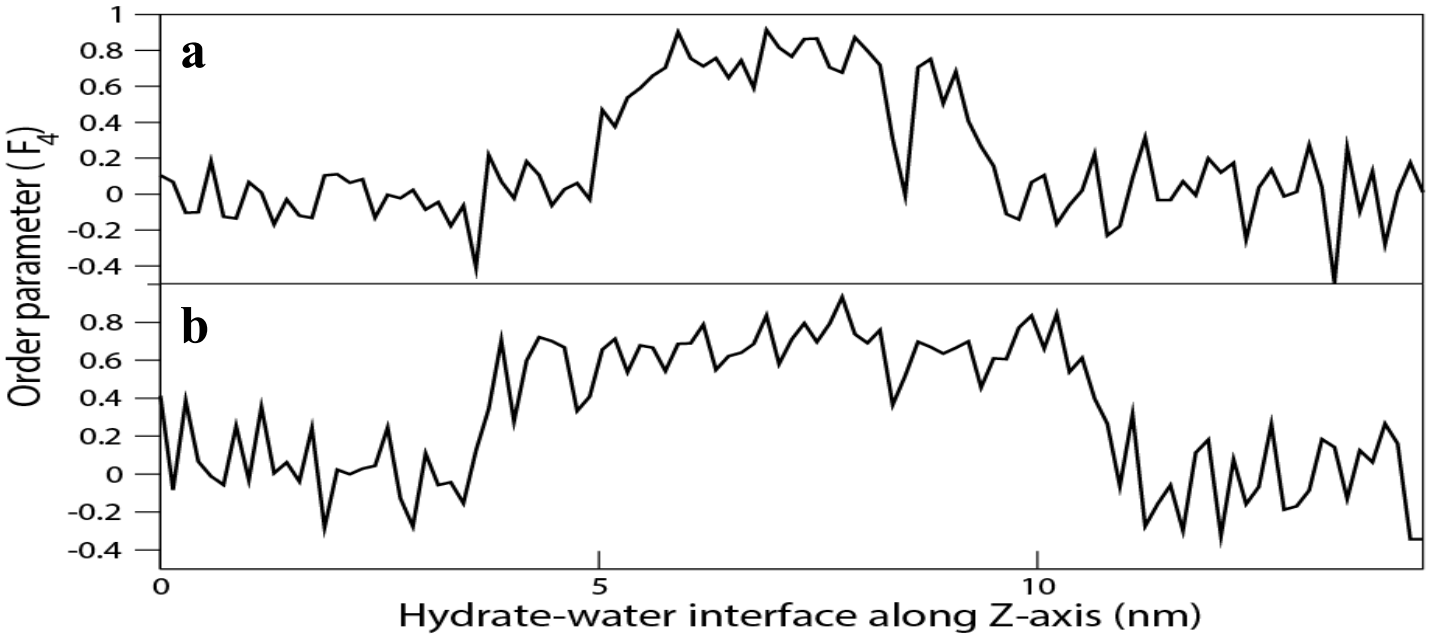

Figure 2: Variation of order parameter along the hydrate water interface (Z-axis) for initial (b) and final (a) at 310K for methane hydrate

Results and Discussions

An interface with amorphous water was created along the Z-axis of the hydrate 3×3×6 supercell on both sides. No guest molecules were present in the bulk water phase (amorphous water) in the initial structure. The guest molecules which came out of the hydrate phase into the bulk phase during the short unrestrained NPT run of 10 ps (at equilibration phase) and during the simulated annealing were not considered for calculation of rate of decomposition. For systems with guest molecules of diameter σ=6.00 Å (maximum size of guest molecule used for simulation see Figure 1), ϵ=1.23 kJ/mol or Helium hydrate (the smallest guest molecule used), some of the guest molecules from the hydrate phase came out into the bulk phase during the short NPT run of 10 ps and also during simulated annealing. Those guest molecules were not considered in the calculations for rate of decomposition. It is considered during the production NVE run as the water cages of the hydrate phase is broken layer by layer causing the guest molecules to come out and get dissolved in the bulk phase[62]. As a result of melting, the interface of the hydrate with the bulk water keeps changing with time. We monitored this change in position of the interfaces by calculating the average structural order parameter of the crystalline and amorphous water phase along the Z-direction i.e., along the direction of interface. The structural order parameter F_4 is defined as

$$F_4 = \frac{1}{n}\sum_{i=1}^{n} \cos 3\phi_i \qquad (2)$$

where n is the oxygen-oxygen pairs of water molecules within 0.3 nm. (The RDF between oxygen atoms of hydrate phase shows the first maximum at 0.3 nm (Figure S3 of ESI)). The angle ϕ is calculated for neighboring oxygen atoms with their outermost hydrogen atoms. Outermost hydrogen atoms were selected by calculating distances between hydrogen atoms and the neighboring oxygen atom. The average value of F_4 for hydrate system and amorphous water are 0.7 and −0.04, respectively[68] . So, the order parameter can be used to distinguish between hydrate phase and the amorphous phase. In

Figure 2a and b, we have shown the F_4 value calculated along the Z-axis at the starting and end of 6ns of NVE run respectively. For calculating F_4, we divided the simulation box in 100 equal slabs along the Z direction. F_4 values were calculated in each of these 100 slabs and averaged for 10ps of initial (Figure 2a) and final NVE run (6 ns) (Figure 2b). The change in interface region is evident from Figure 2a and 2b. In 6 ns of NVE run, the interface gets shifted almost by 1 nm in both the sides of the simulation box (in Z-direction). The same characteristics can be seen for other systems with different guest molecules although the magnitude of the shifting of interface varies from system to system.

Because of the melting of hydrate phase, there is an increase in the pressure and decrease in the temperature of the system. We have shown the temperature and pressure variations for some of the systems with the given guest molecules (σ=3.73 Å, ϵ=1.23 kJ/mol; σ=3.73 Å ϵ=2.3 kJ/mol and σ=3.93 Å ϵ=1.23 kJ/mol) in Figure S4 of ESI. From the temperature variations, we can calculate the equilibrium temperature of the systems under consideration. For calculation of equilibrium temperature, we have used the equation given below by Baghel et al[62]

$$T=T_{eq}+\left(T_0-T_{eq}\right)\exp\left(\frac{KA_s}{m_{w0}C_v}\left(\frac{dN}{dt}\right)t\right) \qquad (3)$$

where T_{eq}=equilibrium temperature T_0 =initial temperature of bulk water K= a arbitrary quantity that is independent of time A_s= cross-sectional area of methane hydrate available for heat transfer from bulk water to methane hydrate m_{w0}=initial mass of bulk water C_v=specific heat of bulk water at constant volume (84 kJ/mol). dN/dt is the number of methane molecules moved out of the hydrate per unit time. Figure 3 represents the equilibrium temperature for different systems calculated by using the equation 3.[62] The experimentally reported equilibrium temperature at 10MPa pressure for methane hydrate is 285K.[25]

Simulation shows that for SI hydrate at 10 MPa, if the size of the guest molecule (σ) is kept constant the equilibrium temperature of hydrates increases with increase in interaction parameter ϵ. Similarly, at a constant interaction parameter ϵ for

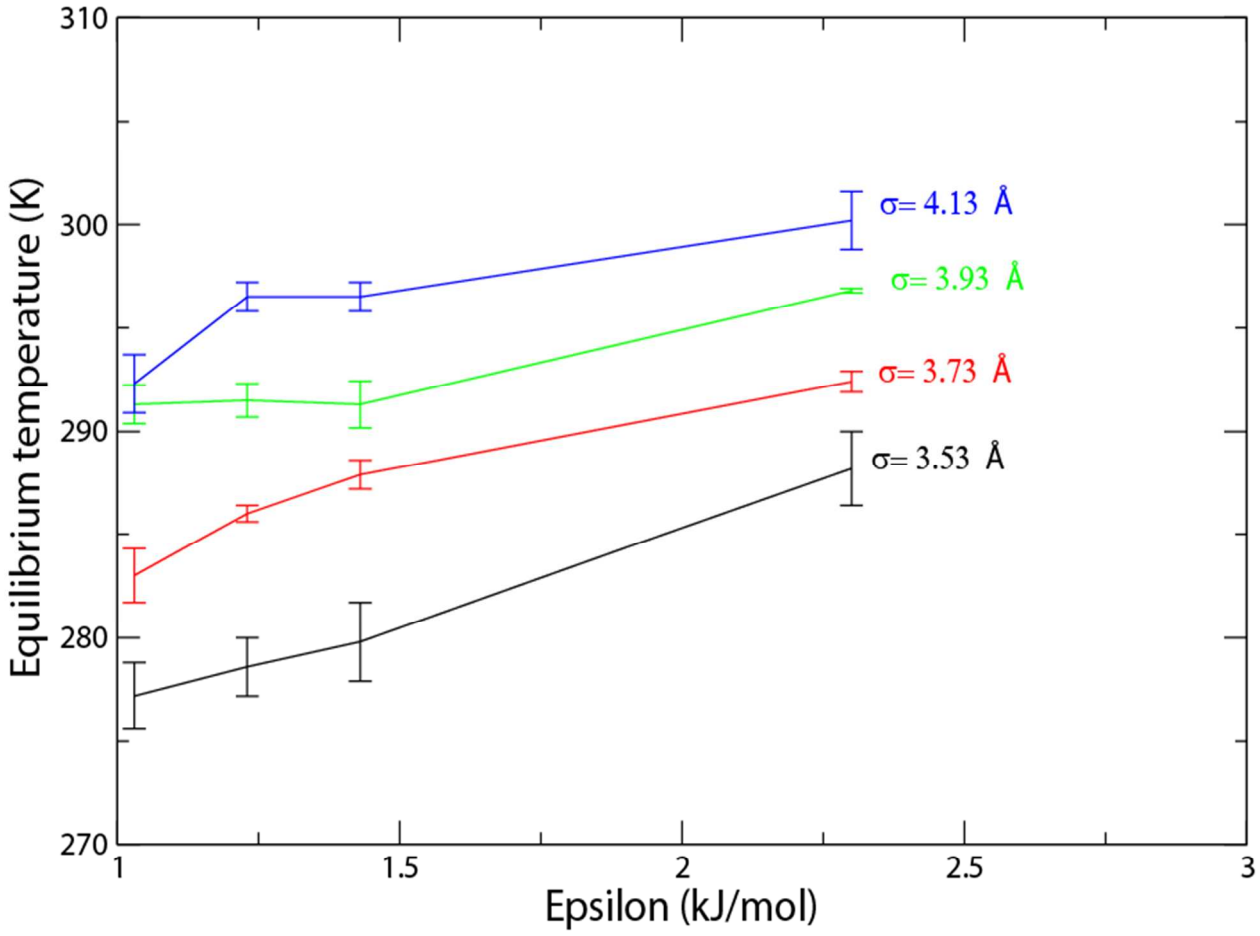

Figure 3. Equilibrium temperature for hydrate with different guest molecules.

Journal Name RSCPublishing

ARTICLE

a guest molecule, the equilibrium temperature for hydrate formation increases with increasing σ. Higher equilibrium temperature at any given pressure indicates higher stability. To correlate equilibrium temperature and stability, we plot the rate of hydrate decomposition (release of guest molecules) during the NVE production run for the systems given at an initial temperature of 310K. Quantification of guest release rate is done by considering a minimum displacement of 0.8 nm of guest molecules in any direction from its starting position in the hydrate cages[60]. From the plots, (Figure S5 in ESI) we see that initial decomposition rate is faster which slows down at a later time probably due to temperature drop brought by decomposing hydrates in an NVE runs. The first part of the plot i.e., faster decay is fitted to a straight line to extract the slope representing the decomposition rate. The decomposition rates as a function of varying sizes σ and interaction parameter ϵ of guest molecule are given in **Figure 4.** This is evident from Figure 4 that there is certain hydrate which decomposes faster (U) compared to others which are slower (S) to decompose.

With slight increase in σ, the rate of decomposition decreases showing better stability. Similarly, increase in ϵ shows slower rate of decomposition thus showing better stability.

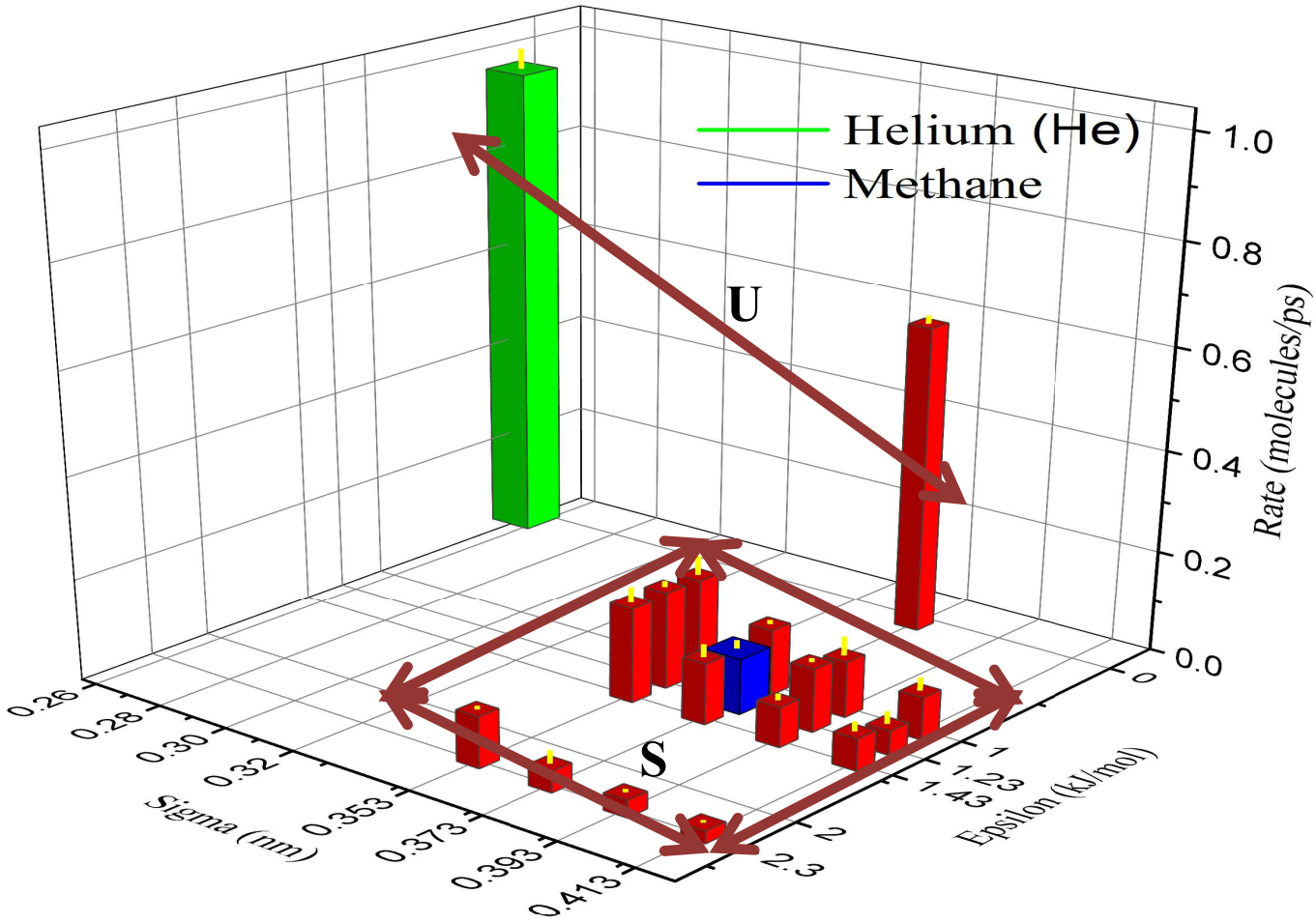

Figure 4. Decomposition rate as function of σ and ϵ at temperature 310K

This is in agreement with Figure 3 where we have shown equilibrium temperature as a function change in the ϵ and σ values.

In Figure 4, the unstable region represent two guest molecules, one is Helium (σ=2.55 Å ϵ=0.08365kJ/mol) and another is model guest molecule with σ same as methane and ϵ

much less than methane (0.083kJ/mol). These two guest molecules represent extreme cases where we see much faster decomposition compared to a comparatively stable SI methane hydrate. To examine how decomposition proceed with large size molecule, we have carried out NVE simulation (following the same protocol as discussed above) for guest molecule with σ= 6.0 Å. In this case, we have kept ϵ same as methane which is 1.23 kJ/mol (not shown in the figure). In Figure 5, we have elucidated snapshots of our simulations on hydrates which fall into stable and unstable zones (see Figure 4). Figure 5a and 5f represents the initial system which was subjected to MD simulation (see computational details) and average partial density (from first 100ps) of hydrate water and guest molecule respectively. In panel b and g of Figure 5, we have depicted a very unstable hydrate system with guest molecule having σ=6.0Å and its partial density respectively. Similarly, in panel d, the snapshot is for guest molecule with ϵ=0.08365 kJ/mol i.e., very small interaction strength with water. From snapshots in panel b and d of unstable hydrates, it is evident that the structures get completely dissociated in the case of guest molecules with less interaction (Figure 5d) and formation of guest molecules clusters can be observed. As expected, guest molecules with higher interaction strength (ϵ=2.3 kJ/mol) shows fairly stable hydrate phase even at 6 ns of NVE simulation (Figure 5e, j). Figure 5c represents hydrate with guest molecules with sigma slightly less than methane (σ=3.73Å) and epsilon same as methane which shows completely decomposed structure at 6ns. In this case, we have also observed formation of clusters of guest molecules. The snapshots of hydrates with σ= 4.13 Å, 3.93 Å, 3.73 Å with constant epsilon of 1.23 kJ/mol and with ϵ=1.43 kJ/mol, 1.03 kJ/mol and constant σ=3.73 Å at 6ns time are given in SI (Figure S6). To understand how hydrates with different guest molecules decompose as a function of time, we have calculated structural order parameter F_4 (as defined in equation 2) from the whole NVE simulation

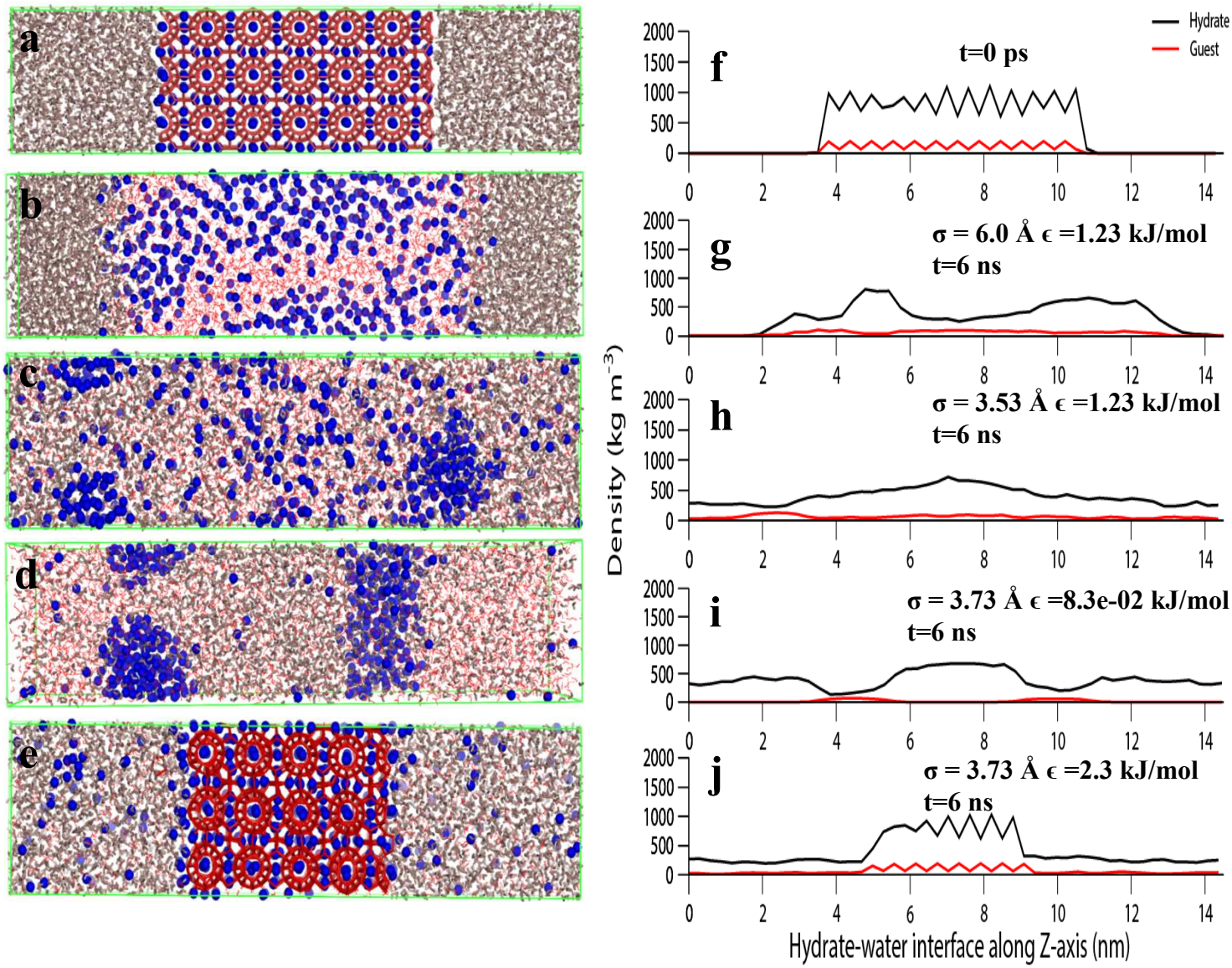

Figure 5: Snapshots of hydrates with different guest molecules at a) the beginning of NVE run after equilibriation, b), c), d) and e) at 6 ns. f), g), h), i) and j) corresponding partial densities for hydrate water and guest molecules.

trajectory. The F_4 order parameters are calculated only for hydrate water molecules. In Figure 6, we have plotted F_4 as a function of time for hydrate with guest molecules with varying sigma and constant epsilon (1.23 kJ/mol). It is clear from Figure (6a) that a molecule of same interaction strength as methane but slight bigger in size (4.13 Å) shows stable hydrate region upto 6ns of simulation. However, a guest molecule of similar as methane but slightly smaller in size (σ=3.53 Å) has lesser stability that methane and decomposes faster. In other words a molecule like CO_2 which is slightly larger than methane has better kinetic stability compared to methane for In Figure 6b, we have shown two extreme cases (σ=6.0 Å and Helium σ=2.55 Å). In both the cases decomposition happens in initial few picosecond indicating unstable hydrate. These systems

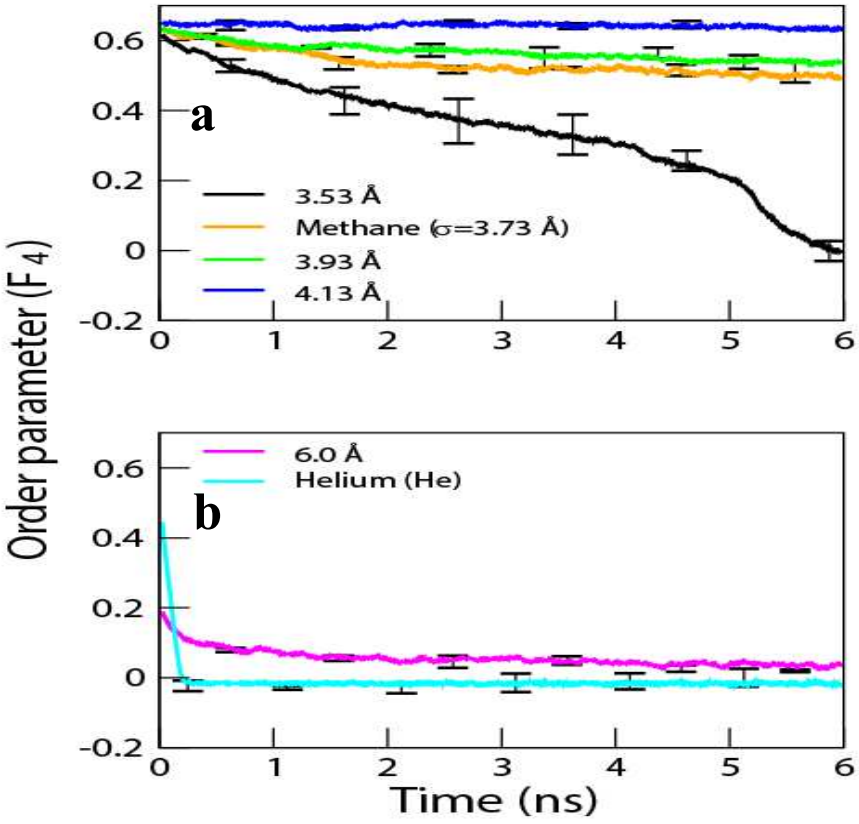

Figure 6. Order parameter as a function of time for hydrate with guest molecules with different sigma but constant epsilon (1.23 kJ/mol) for a) stable b) unstable zone (see Figure 4).

even decomposed to certain extent at equilibrium steps of MD simulation. It clearly shows that guest size to cage ratio is an important parameter and contribute significantly to hydrate stability. The effect of interaction of guest molecule with hydrate cage become prominent when we calculate F_4 parameter as a function of simulation time for systems with varying epsilon and constant σ (3.73 Å). Figure 7 depicts the decay of F_4 order parameter as a function of time for hydrate with different epsilon. Guest molecule with ϵ=2.3 kJ/mol which is more attractive towards water than methane stabilizes the hydrate structure till 6 ns of simulation time at 310K. This clearly shows that higher hydrophilicity of CO_2 (i.e., stronger interaction toward water) helps the SI stability compared to methane hydrate. From Figure 5e, j we have also seen partial decomposition of hydrate with the guest molecule with higher interaction strength than methane. However, hydrate with guest molecule which has lower epsilon than methane decomposes much faster than methane hydrate. From Figure 7b, it is evident that a guest molecule with less interaction strength (where ϵ =0.083 kJ/mol σ=3.73 Å)

and Helium gas starts decomposing in the initial few picosecond of MD simulation run. From Figure 6 and 7, it was concluded that guest molecules with higher interaction strenght than methane and with slightly larger in size than methane can stabilize structure I at 310K and CO2 fits this description quite

well. However, it is known that in SI hydrate CO_2 partially occupies the hydrate cages and thus may contribute to kinetic unstability once such hydrate starts decomposition. We did not show any data resulted from simulation at 300K because of similarity in trends with 310K data. We have further verified the stability of hydrates with different guest molecules by calculating potential energy experienced by guest molecules at the interface, bulk and hydrate phases as a function of simulation time at 310 K. To calculate these energies, we have divided the simulation box in twelve equal slabs along hydrate-water interface (Z-axis) as shown in Figure S7 of SI. As shown in Figure 2 reported by Baghel et al, hydrate phase decomposes layer by layer starting from the interface. Therefore, to track the change of hydrate-water interface as a function of time,

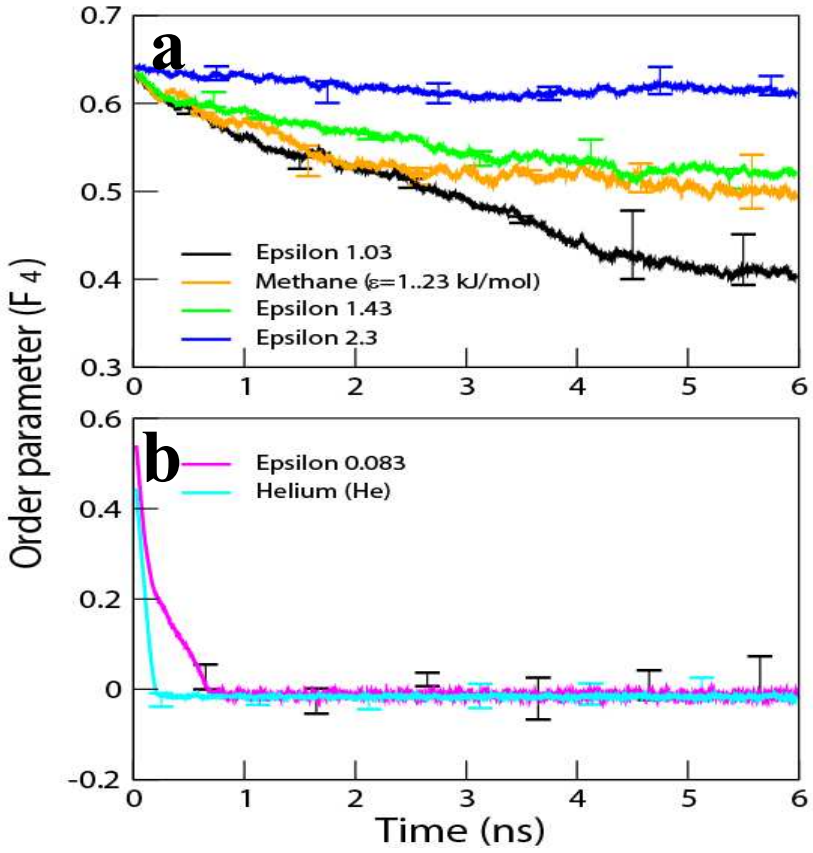

Figure 7 Order parameter as a function of time for hydrate with guest molecules with different epsilon but constant sigma (3.73 Å) for a) stable b) unstable zone (see Figure 4).

we have calculated average structural order parameter (F_4) for water molecules in these slabs. We have assigned the interface slabs where we have observed maximum change in F_4 value (bulk water to hydrate phase change of F_4 value is from 0 to 0.64). Slabs for bulk and hydrate water phase are also assigned by calculating F_4 value. Guest molecules present in these phases experience potential energy from all other molecules of the simulation box. Therefore, we have calculated total non-bonded interactions per guest molecule in each phase and plotted in Figure 8 as a function of time. The total non-bonded potential energy is calculated as a sum of LJ between guest-guest and guest-water molecules. Finally, total non-bonded energy was divided by number of guest molecules in that particular phase (dynamically defined slabs). It is evident from the Figure 8 that slight increase in sigma from methane (σ= 3.73 Å) guest molecules experiences higher stability (lower potential energy) in the hydrate and interface region. However guest molecules with lower sigma than methane destabilizes the hydrate phase the most. Similarly, with an increase in epsilon of guest molecules (which may be correlated with hydrophilicity)

guest molecules experiences lower potentials energy in hydrate phase, which stabilizes the hydrate. In some cases the energies go to zero, which signify the absence of hydrate phase because of complete decomposition and nonexistence of guest molecules in the bulk phase at the beginning of the simulation. Figure 8 clearly shows the how the interaction between guest and water molecules plays a significant role in stabilizing the hydrate.

Conclusions

Decomposition of SI hydrate in presence of model guest molecules with different size and interaction strength with water at 310 K was studied and the decomposition kinetics was compared with methane hydrate decomposition. The LJ parameters for guest molecules have been changed systematically and independent MD simulations were carried out. The size of the guest molecules is defined by the LJ parameter sigma and interaction by epsilon. Double-precision GROMACS code is used to study the decomposition of fully occupied SI hydrate with model guest molecules by employing NVE - MD simulations using SPC/E water models. For improved statistics each simulation was repeated thrice and the data was reported with error bars. We have observed early decomposition of hydrate with guest molecules sized lower

Journal Name RSCPublishing

ARTICLE

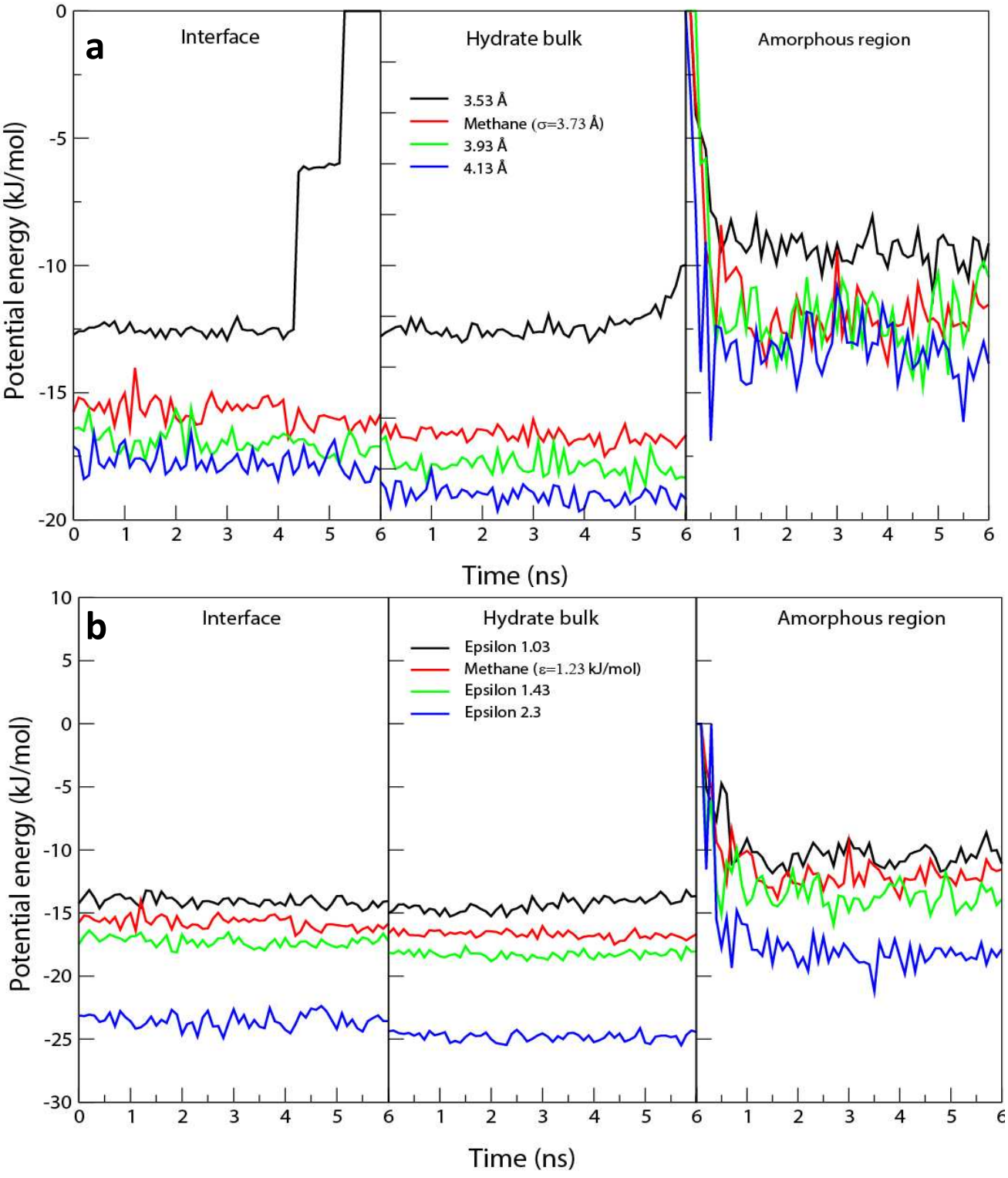

Figure 8 Potential energy felt by guest molecules in interface, hydrate phase and bulk water phase as a function of time for

hydrate with guest molecules a) with different sigma but constant epsilon (1.23 kJ/mol) b) with different epsilon but constant sigma (3.73 Å).

,than methane. Guest molecules with sigma (size) higher than methane increases the stability of the hydrate to certain extent. However, guest molecules much larger in size than the cage diameter of SI hydrate resulted in immediate decomposition. We have quantified the rate of decomposition by calculating number of guest molecules coming out of hydrate cages as function of time. From these calculations we can conclude that molecules, which are slightly larger in size and more hydrophilic than methane, are more stable than methane hydrate. We have verified this by calculating structural order parameter (F_4) for hydrate with different guest molecules as a function of time. This work clearly shows replacement of methane hydrate with CO_2 molecule would lead to a more stable system, thus making the molecular replacement approach quite feasible. H_2S is another guest molecule candidate, which might also replace CH_4 from natural gas hydrates.

Acknowledgements

The author SD would like to thank CSIR, India, for providing fellowship. SR gratefully acknowledges the Center for Excellence in Scientific Computing, NCL (project code CSC0129), for financial support and computational time. RK acknowledges the funding support from CO_2 capture program under TAPCOAL project (CSC 0102). The authors sincerely thank Dr. Prithvi Raj Pandey for his valuable guidance and discussion. We greatly acknowledge the computational support given by CSIR Fourth Paradigm Institute (CSIR-4PI)– Bangalore for providing computational resources and support.

Notes and References

[a] Physical Chemistry Division, National Chemical Laboratory.
[b] Chemical engineering and process developmemt, National chemical Laboratory

† Electronic Supplementary Information (ESI) available: Snapshots of some of the model guest molecule hydrates, pressure, temperature and total energy plots are given;. See DOI: 10.1039/b000000x/

1. E. D. Sloan and C. A. Koh, *Clathrate Hydrates of Natural Gases*, CRC Press, Taylor & Francis Group, Boca Raton, FL, 3rd ed. edn., 2008.
2. B. A. Buffett, *Annual Review of Earth and Planetary Sciences*, 2000, 28, 477-507.
3. H. D. J. Davy, *The collected works of Sir Humphry Davy*, Thoemmes, Bristol, 2001.
4. E. G. Hammerschmidt, *Industrial & Engineering Chemistry*, 1934, 26, 851-855.
5. T. S. Collett, *AAPG Bulletin*, 1993, 77, 793-812.
6. E. D. K. C. A. Sloan, *Clathrate hydrates of natural gases*, CRC Press, Boca Raton, Fla. [u.a., 2008.
7. R. Kumar, D. D. Klug, C. I. Ratcliffe, C. A. Tulk and J. A. Ripmeester, *Angewandte Chemie International Edition*, 2013, 52, 1531-1534.
8. R. Kumar, P. Linga, J. Ripmeester and P. Englezos, *Journal of Environmental Engineering*, 2009, 135, 411-417.
9. L. J. Florusse, C. J. Peters, J. Schoonman, K. C. Hester, C. A. Koh, S. F. Dec, K. N. Marsh and E. D. Sloan, *Science*, 2004, 306, 469-471.
10. H. Lu, J. Wang, C. Liu, C. I. Ratcliffe, U. Becker, R. Kumar and J. Ripmeester, *Journal of the American Chemical Society*, 2012, 134, 9160-9162.
11. H. P. Veluswamy, R. Kumar and P. Linga, *Applied Energy*, 2014, 122, 112-132.
12. H. P. Veluswamy and P. Linga, *International Journal of Hydrogen Energy*, 2013, 38, 4587-4596.
13. T. A. Strobel, K. C. Hester, C. A. Koh, A. K. Sum and E. D. Sloan Jr, *Chemical Physics Letters*, 2009, 478, 97-109.
14. J. Javanmardi and M. Moshfeghian, *Applied Thermal Engineering*, 2003, 23, 845-857.
15. K.-n. Park, S. Y. Hong, J. W. Lee, K. C. Kang, Y. C. Lee, M.-G. Ha and J. D. Lee, *Desalination*, 2011, 274, 91-96.
16. A. Kumar, T. Sakpal, P. Linga and R. Kumar, *Fuel*, 2013, 105, 664-671.
17. P. Babu, R. Kumar and P. Linga, *International Journal of Greenhouse Gas Control*, 2013, 17, 206-214.
18. S. R. Zele, S. Y. Lee and G. D. Holder, *The Journal of Physical Chemistry B*, 1999, 103, 10250-10257.
19. Y.-T. Tung, L.-J. Chen, Y.-P. Chen and S.-T. Lin, *The Journal of Physical Chemistry B*, 2010, 114, 10804-10813.
20. H. Nada, *The Journal of Physical Chemistry B*, 2009, 113, 4790-4798.
21. S. Liang and P. G. Kusalik, *The Journal of Physical Chemistry B*, 2010, 114, 9563-9571.
22. S. Liang and P. G. Kusalik, *Chemical Physics Letters*, 2010, 494, 123-133.
23. J. Vatamanu and P. G. Kusalik, *The Journal of Physical Chemistry B*, 2006, 110, 15896-15904.
24. S.-H. Park and G. Sposito, *The Journal of Physical Chemistry B*, 2003, 107, 2281-2290.
25. N. Goel, *Journal of Petroleum Science and Engineering*, 2006, 51, 169-184.
26. in *Clathrate Hydrates of Natural Gases, Third Edition*, CRC Press, 2007, DOI: doi:10.1201/9781420008494.ch2, pp. 45-111.
27. K. Tezuka, K. Murayama, S. Takeya, S. Alavi and R. Ohmura, *The Journal of Physical Chemistry C*, 2013, 117, 10473-10482.
28. M. B. Rydzy, J. M. Schicks, R. Naumann and J. r. Erzinger, *The Journal of Physical Chemistry B*, 2007, 111, 9539-9545.
29. R. A. Kini, Huo, Z., Jager, M.D., Bollavaram, P., Ballad, A.L., Dec, S.F., Sloan, Icgh International Conference on Gas Hydrates, Yokohama, 2002.
30. K. A. Udachin, Ratcliffe, C.I., Ripmeester, J.A., Icgh International Conference on Gas Hydrates, Yokohama, 2002.
31. G. D. Holder, S. Zele and R. Enick, *Annals of the New York Academy of Sciences*, 1994, 715, 344-353.
32. T. Uchida, R. Ohmura and A. Hori, *The Journal of Physical Chemistry C*, 2008, 112, 4719-4724.
33. Y. Liu, J. Zhao and J. Xu, *Computational and Theoretical Chemistry*, 2012, 991, 165-173.
34. M. Ota and Y. Qi, *JSME International Journal Series B*, 2000, 43, 719-726.
35. L. A. BÁEz and P. Clancy, *Annals of the New York Academy of Sciences*, 1994, 715, 177-186.
36. R. Radhakrishnan and B. L. Trout, *The Journal of Chemical Physics*, 2002, 117, 1786-1796.
37. N. J. English, J. K. Johnson and C. E. Taylor, *The Journal of Chemical Physics*, 2005, 123, 244503-244512.
38. N. J. English and J. M. D. Macelroy, *Journal of Computational Chemistry*, 2003, 24, 1569-1581.
39. R. M. Pratt, D.-H. Mei, T.-M. Guo and J. E. D. Sloan, *The Journal of Chemical Physics*, 1997, 106, 4187-4195.
40. P. M. Rodger, *Annals of the New York Academy of Sciences*, 2000, 912, 474-482.
41. V. Chihaia, S. Adams and W. F. Kuhs, *Chemical Physics*, 2005, 317, 208-225.
42. R. E. Westacott and P. M. Rodger, *Chemical Physics Letters*, 1996, 262, 47-51.

43. R. E. Westacott and P. M. Rodger, *Journal of the Chemical Society, Faraday Transactions*, 1998, 94, 3421-3426.
44. C. Moon, P. C. Taylor and P. M. Rodger, *Journal of the American Chemical Society*, 2003, 125, 4706-4707.
45. O. K. Forrisdahl, *Molecular Physics*, 1996, 89, 819-834.
46. H. Nada, *The Journal of Physical Chemistry B*, 2006, 110, 16526-16534.
47. L. Y. Ding, C. Y. Geng, Y. H. Zhao and H. Wen, *Molecular Simulation*, 2007, 33, 1005-1016.
48. H. Jiang and K. D. Jordan, *The Journal of Physical Chemistry C*, 2010, 114, 5555-5564.
49. E. M. Myshakin, H. Jiang, R. P. Warzinski and K. D. Jordan, *The Journal of Physical Chemistry A*, 2009, 113, 1913-1921.
50. Y. Iwai, H. Nakamura, Y. Arai and Y. Shimoyama, *Molecular Simulation*, 2009, 36, 246-253.
51. B. Hess, C. Kutzner, D. van der Spoel and E. Lindahl, *Journal of Chemical Theory and Computation*, 2008, 4, 435-447.
52. H. J. C. Berendsen, J. R. Grigera and T. P. Straatsma, *The Journal of Physical Chemistry*, 1987, 91, 6269-6271.
53. M. P. Allen and D. J. Tildesley, *Computer simulation of liquids*, Clarendon Press, 1989.
54. P. P. Ewald, *Annalen der Physik*, 1921, 369, 253-287.
55. T. Darden, D. York and L. Pedersen, *The Journal of Chemical Physics*, 1993, 98, 10089-10092.
56. U. Essmann, L. Perera, M. L. Berkowitz, T. Darden, H. Lee and L. G. Pedersen, *The Journal of Chemical Physics*, 1995, 103, 8577-8593.
57. J. D. Bernal and R. H. Fowler, *The Journal of Chemical Physics*, 1933, 1, 515-548.
58. V. S. Baghel, R. Kumar and S. Roy, *The Journal of Physical Chemistry C*, 2013, 117, 12172-12182.
59. M. Parrinello and A. Rahman, *Journal of Applied Physics*, 1981, 52, 7182-7190.
60. S. Nosé and M. L. Klein, *Molecular Physics*, 1983, 50, 1055-1076.
61. B. Hess, C. Kutzner, D. van der Spoel and E. Lindahl, *Journal of Chemical Theory and Computation*, 2008, 4, 435-447.
62. C. Moon, R. W. Hawtin and P. M. Rodger, *Faraday Discussions*, 2007, 136, 367-382.
63. S. Alavi and J. A. Ripmeester, *The Journal of Chemical Physics*, 2010, 132, 144703-144708.

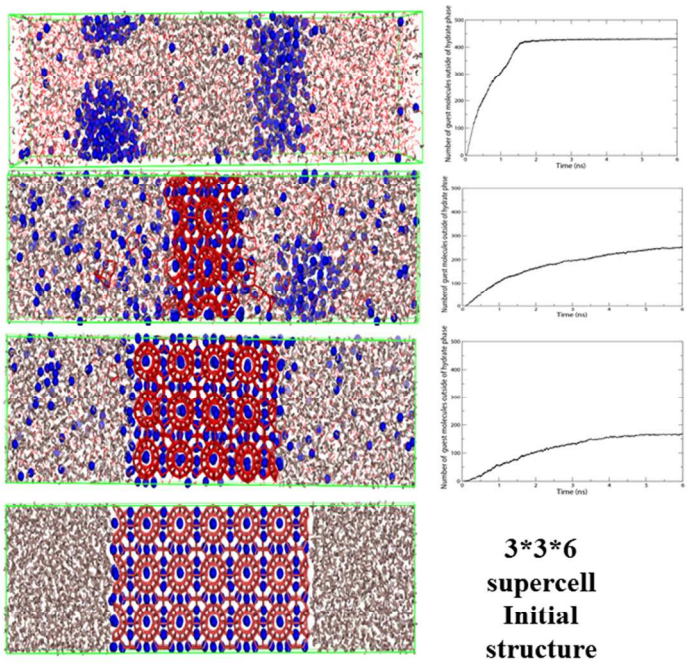

Graphical Abstract
254x190mm (96 x 96 DPI)